Proc. IEEE MFI, pp.15–21, Aug. 2003.

Development of Artificial Finger Skin to Detect Incipient Slip for Realization of Static Friction Sensation

Isao Fujimoto, Yoji Yamada
Tetsuya Morizono, Yoji Umetani
Intelligent Systems Laboratory
Toyota Technological Institute
2-12-1, Hisakata, Tenpaku-ku
Nagoya 468-8511, Japan

Takashi Maeno

Department of Mechanical Engineering
Keio University
3-14-1, Hiyoshi, Kohoku-ku
Yokohama 223-8522, Japan

Abstract

The goal of our study is realization of static friction sensation using a piece of artificial finger skin for robot hand manipulation. In order to realize the sensation, we recall the importance of incipient slip detection. First, artificial finger skin is designed which is mimicked to have characteristics similar to that of a human finger with respect to the shape and a part of the sensing functions which such enable the incipient slip detection: The finger skin has ridges on the surface in each of which a pair of artificial **FAI** *receptors are embedded. The design process of artificial finger skin is also shown that includes three phases. Design phase ♯1 is to design the characteristics of a* **FAI** *receptor as the transducer of which, we choose PVDF film sheets which have a dynamic stress rate characteristic. Design phase ♯2 involves determination of the shape and size of artificial finger skin, and the location of the transducers in a ridge. We analyze the stress in the finger skin when incipient slip occurs at the surface. The signal from transducer is analyzed what the best situation of the position of transducer and the using information of transducer at the future process. Design phase ♯3 is to manufacture artificial finger skin. Experimental result that incipient slip occurs at the surface of artificial finger skin reveal that the differential output voltage signal from a pair of artificial* **FAI** *receptors embedded in a ridge captures not only low-frequency vibration to generate a predictive signal which warns incipient slip of the ridge, but also high frequency vibratory signal which indicates slip of the ridge. In order to judge automatically that incipient slip occurs we use multi-layered ANN. The result to judge incipient slip use ANN shows that the system is robust to noise and can detect the incipient slip.*

1 Introduction

Most of the conventional approaches to construction of various robot tactile sensor mechanisms hold a fundamental problem of a spatial limitation when they are attempted to be mounted on a small area of a robot fingertip for integration of their individual functions. This is because the limited space at a robot fingertip cannot house many sensor mechanisms without causing any mechanical interference with one another. By contact, various kinds of human tactile perception are attained through integrated processing of tactile information from only several kinds of mechanoreceptors. Therefore, we consider it very important to build a tactile sensing system based upon a design policy of taking the behavior of tactile sensing elements and the tissue embedding them at the same time. Consequently, it becomes worth notice to realize artificial finger skin with sensing elements incorporated into the skin tissue so that they can be expected to have various robot tactile perception capabilities under a novel platform concept: the sensing elements should have a wider frequency detectable range and acquire meaningful information by their elaborate spatial allocation. In the study, we demonstrate the effectiveness of this design policy by pursuing incipient slip detection which plays an important role in elucidating the static friction sensation mechanism.

For this purpose, we decided to attain vibrotactile sensing capabilities on a skin tissue that has softness like humans. Early, Johansson et al.[1] examined in their study of human static friction sensation that a parallel change in the grip and the load forces is observed during precision grip of an object and the ratio between two forces is adapted to result in the static friction coefficient between the finger skin surface and the object. According to their suggestion that incipient slip information should play an important role in such precision grip, several studies on robotic incipient slip detection have been reported. Gaetano et al.[2] proposed a tactile sensor system capable of detecting the incipiency of slip between an object and the sensor surface using the normal and shear stress information from arrays of PVDF transducers. They showed by both simulation and experimentation that a trained neural network with the normal and shear stress signal patterns allowed them to find the incipient slip. However, this method is different from the standard detecting method of incipient slip: An object in contact with a rubber surface is slid on a curved surface and the peripheral area of the contact is initiated to slip.

In this respect, Tremblay et al.[3] demonstrated the effectiveness of incipient slip detection more early using the peripheral slip signal from accelerometers which were mounted on a curved soft surface.

Similarly, J. S. Son et al.[4] also devised the surface of the rubber skin to have molded surface texture with arrayed tiny nibs for the purpose of easily obtaining the incipient slip. However, we can still design better shape and struc-

ture of the skin surface ridges with vibrotactile sensing elements because the mechanical behavior of nibs and the directivity of the sensors are not necessarily optimized in the above two proposals due to their separate allocation. As the background of establishing a novel design strategy, we have studied the dynamic response of human finger skin for tactile receptors focusing on the effect of epidermal ridges using FE analysis[5]. We have also proposed to detect impulsive high-frequency vibratory signal at robotic finger surface ridges where PVDF film strips are embedded for isolating a slip phase from various other contact phases[6].

Moreover, what kind of transducers with 20 dB/dec or higher order dynamic sensing characteristics we should use is also an important technical issue. Though the above approach by Tremblay et al. to using accelerometers is considered to have higher sensitivity in acquiring vibrotactile information, they cannot be easily downsized. PVDF film transducers which were introduced to this study field by Dario et al.[7] are promising due to their flexibility and high sensitivity. Later work on texture distinguishment by Patterson et al.[8] is also notable, from the viewpoint that the work was the first proposal of using the PVDF film transducers in dynamic tactile sensing which is a widely applicable concept developed by Howe et al.[9]. They also used the same PVDF film transducers referring to it as stress rate sensor in their work on monitoring contact conditions for dextrous robot hand manipulation. It is interesting to note that a PVDF transducer has the possibility of exhibiting various frequency characteristics in connection with an amplifier[10].

In this study, we show a development process of artificial finger skin surface ridges in each of which a pair of PVDF film strips are embedded. The design process of artificial finger skin regarding the shape and size is described in **chapter 2**. In **chapter 3**, the frequency characteristic of a PVDF circuit is examined with the equivalent circuit modeled. In **chapter 4**, artificial finger skin is designed mimicking human digital skin. In **chapter 5**, artificial finger skin is manufactured and we demonstrate that the sensing function of artificial finger skin allows us to detect the incipient slip. In **chapter 6**, multi-layered ANN is applied to judgment of incipient slip generation using transducer signal. The conclusion for this study is finally made in **chapter 7**.

2 Design Processes of Artificial Skin

There are two processes of designing artificial finger skin for this study, which are schematically described in **Figure 1**. The first process **A** consists of three design phases; design ♯1, ♯2 and ♯3. Design phase ♯1 is to examine the frequency characteristics and the sensitivity of the transducer circuit used in artificial finger skin. We select PVDF film as the transducer of artificial mechanoreceptors because the film has high mechanical flexibility and we can expect high sensitivity of piezoelectricity with dynamic responses of technical interest. We consider that this phase of determining the equivalent circuit of the PVDF film in connection with an amplifier is important for later use of designing more desired PVDF transducer circuits. In design phase ♯2, we design the shape and size of artificial finger skin. In this phase, it is important to identify where the PVDF transducers should be localized and what kind of tactile information from the transducers is significant in detecting incipient slip. The above two design phases are conducted independently, and design phase ♯3 connect these two phases. In this phase, artificial finger skin is manufactured and analyzed mechanism of our main concern that incipient slip occurs at the surface of the artificial finger skin. We analyze the signal from artificial mechanoreceptors and consider how to detect the incipient slip at the surface of the skin. Design process **B** will be the future work to consider after taking the design process **A** into account to seek for an optimal solution to artificial finger skin with more highly sensitive and reliable incipient slip detection capability.

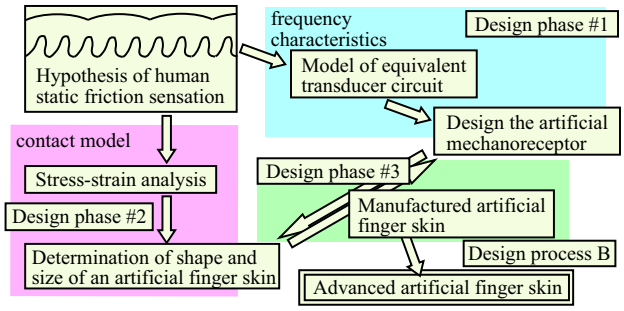

Figure 1: Design process of artificial finger skin

In order to realize the static friction sensation, restriction is given from the following two keys features which we hypothesize from an engineering viewpoint. First, the sensation can be realized principally by detection of incipient slip. Second, **FAI** is the mechanoreceptor in the human digital skin that plays the major role of incipient slip detection.

3 Design phase ♯1: Examination of the frequency characteristic of a PVDF circuit

3.1 A circuit model

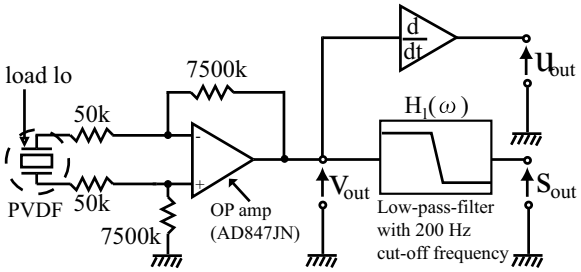

Figure 2: Circuit diagram of a PVDF circuit (a PVDF transducer + a differential amplifier) + signal processing

Figure 2 is a schematic of a PVDF circuit we made for our study, which is composed of a PVDF film transducer followed by a differential amplifier. The output signal v_{out} of a differential amplifier is connected to a low-pass filter with a cut-off frequency $f_c = 200$ Hz and the filtered signal s_{out} is obtained. The amplitude characteristic of the low-pass filter is expressed as

$$|H_l(\omega)| = \frac{1}{1 + (\frac{\omega}{400\pi})^2} \tag{1}$$

where $\omega = 2\pi f$, and f is frequency. The signal u_{out} is obtained that v_{out} is differentiated. The differential amplifier, which is mainly a high input impedance operational amplifier OP amp and plays an important role of rejecting common mode noise, is connected to a PVDF film transducer.

A load *lo* is applied to the PVDF transducer. It generates electric charges which are converted to output voltage v_{out} by the succeeding differential amplifier. We can monitor the four parameters *lo*, v_{out}, s_{out} and u_{out}, and compute the *Gain* of the linear PVDF circuit system which is defined as

$$Gain(*_{out}) = 20 \log_{10} \left| \frac{*_{out}}{lo} \right| \qquad (* = v, s, u) \tag{2}$$

where $Gain(*_{out})$ is a function of frequency $f = \omega/2\pi$ because the PVDF circuit exhibits a dynamic characteristic due to the parallelly connected CR equivalent circuit components of both the PVDF film and the OP amp input.

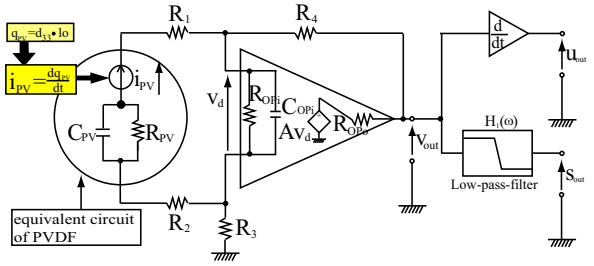

Figure 3: Overall equivalent circuit of the PVDF circuit

Figure 3 shows the overall equivalent circuit diagram including that of the succeeding OP amp[13]. Electric charge q_{PV} induced at the electrodes of a polarized PVDF transducer due to the applied stress results from free electrons existing in the vicinity of the electrodes. q_{PV} is proportional to the applied stress *lo*,

$$q_{PV} = d_{33} lo \tag{3}$$

where d_{33} is the piezoelectric strain constant: d_{33} means the ratio of the charges generated in the 3-axis (in the direction of film thickness) when unit mechanical stress is applied to the same 3-axis.

Solving the linear simultaneous equations for the circuit system in **Figure 3**, the PVDF circuit gain is formulated as

$$Gain(v_{out}) = 20 \log_{10} \left| (R_{OPO} + A_4) \frac{d_{33} j\omega e^{j\omega t}}{A_3 A_2} \right| \tag{4}$$

where A_2 through A_4 in formula (4) are developed as follows.

$$A_2 = \frac{R_{OPO}}{R_{OPi} + R_1 + R_2 + R_{PV}(1 - A_1)} \tag{5}$$

$$A_3 = \frac{1}{j\omega C_{OPi} R_{OPi}(1 - A_2) + 1} \tag{6}$$

$$A_4 = \frac{j\omega C_{OPi}}{1 - A_3 + j\omega C_{OPi}(R_3 + R_4 + R_{OPO})} \tag{7}$$

where A_1 is:

$$A_1 = \frac{j\omega C_{PV} R_{PV}}{1 + j\omega C_{PV} R_{PV}} \tag{8}$$

3.2 Experimental setup

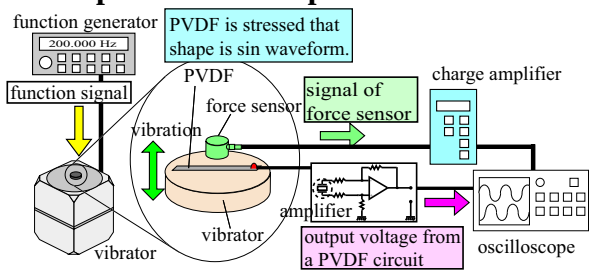

Figure 4: Experimental setup for examining the frequency characteristic of a PVDF circuit

The experimental setup for examining the frequency characteristics of a PVDF circuit is shown in **Figure 4**. The PVDF film (Kureha Chemical Industry Co.: KF Piezofilm) is preloaded at 20 N between the indentor of a vibrator (IMV Co.: PET-05) and a force sensor probe (KISTLER CO.: 9213A1). The film is a strip-shaped with 30 mm length, 2 mm width and 80 μm thickness. The area of the contact plane between the film surface and the indentor is 8.7 mm^2. The vibrator is driven by a sinusoidal input signal. The magnitude of the sinusoidal load *lo* is 4 N which is observed by a force sensor, and is kept constant regardless of the input frequency f which ranges from 10 to 1000 Hz. Ten PVDF films are explained to detect *Gain* as same condition.

3.3 Experimental results

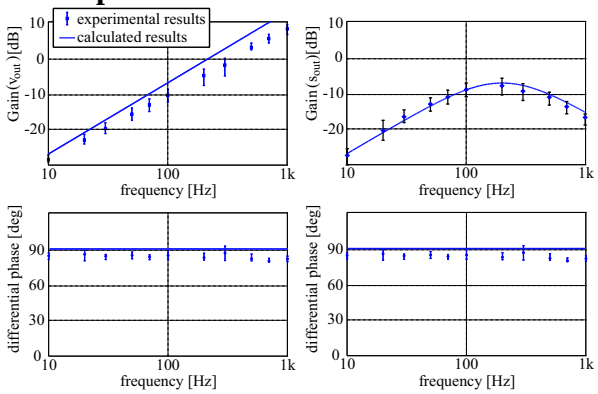

(a) v_{out} (b) s_{out}

Figure 5: Experimental result

Experimental results of the frequency characteristics of a PVDF circuit are shown in **Figure 5**. We obtain the experimental results from ten samples for each plot of frequency.

Table 1: Calculated parameter

C_{PV}	3.0×10^{-11}[F]	C_{OPi}	1.5×10^{-12}[F]
R_{PV}	8.0×10^{5}[Ω]	R_{OPi}	3.0×10^{5}[Ω]
		R_{OP0}	15[Ω]

Calculated results of *Gain* obtained from (4) through (8) are plotted as the dotted lines in **Figure 5** by use of the circuit parameters in **Table 1**.

Figure 5(a) shows the experimental result of $Gain(v_{out})$ which indicates a linear characteristic to be expressed as

$$Gain(v_{out}) = a\log_{10}|f| + b \tag{9}$$

where a and b are constant parameters which are experimentally identified as $a = 18.4$ dB/dec, $b = -46.9$ dB. On the other hand, constants of the calculated results of $Gain(v_{out})$ are $a = 20.0$ dB/dec, $b = -46.8$ dB. There is 1% significance of constant a between the calculated and the experimental results. Frequency characteristics of filtered output $Gain(s_{out})$ is shown in **Figure 5(b)**. The result shows a band-pass characteristic with 200 Hz peak frequency.

4 Design phase ♯2: Design of artificial finger skin

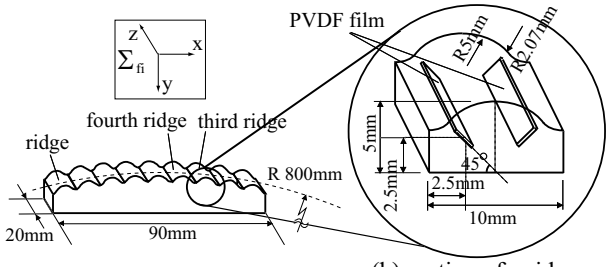

Figure 6: Design of artificial finger skin

In design phase ♯2, we manufactured an artificial finger skin piece whose shape and size are designed as shown in **Figure 6**[11]. **Figure 6(a)** shows the overall skin piece with nine ridges, and the detail of one ridge is shown in **Figure 6(b)**. We designed the artificial finger skin piece imitating the following characteristics of human fingers. First, tissue of a human finger except for bones consists of flexible materials. The materials transform contact information to tactile receptors through elastic deformation of the tissue. Second, a human finger has a curved surface in broad perspective. Third, epidermal ridges are distributed at a finger surface. A pair of **FAI** receptors is observed to be located at the top dermis papilla underneath one epidermal ridge [12]. It is analyzed by FEM that all of the nine ridges contact a flat object when normal force of 4 N is applied.

5 Design phase ♯3: Manufacture artificial finger skin and experiment of incipient slip

5.1 Experimental setup for generating incipient slip

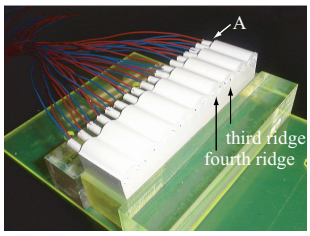

Figure 7: Picture of the manufactured artificial finger skin

Figure 7 is a photograph of the manufactured skin piece of 20 mm width, which consists of silicone rubber (Shinetsu silicone: KE12). There are two PVDF film strips of 30 mm length in the ridge. The glued parts are **A** as shown in the figure. A PVDF film strip is longer than the width of the skin piece because the glued connection parts between the PVDF strip electrodes and signal wires are harder than the silicone rubber material: If the harder part was in artificial finger skin, mechanical behavior in artificial finger skin would be changed. The artificial finger skin was fixed to a thick acrylic substrate.

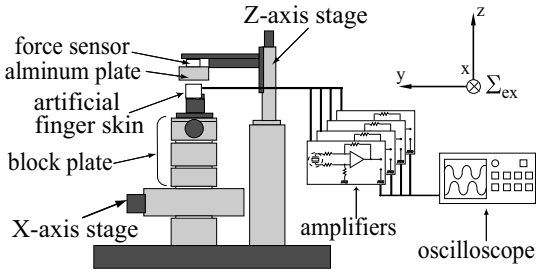

Figure 8: Experimental setup to examine incipient slip detection performance

The experimental setup for examining the performance of incipient slip detection is shown in **Figure 8**. As shown in the figure, artificial finger skin is fixed to a block plate which is driven in the x and z directions by a x-z stage. The skin is sensitive to slip incipiency in the x direction. The aluminum plate which is in contact with the skin surface at constant normal force is slid in the x direction. Two signal channels of the output voltage from the third and fourth elements are monitored at 10 kHz sampling rate.

5.2 Experimental results

We define the name of PVDF film shown in the **Figure 9** and output signals $v_{out}^{\sharp A-1}$, $s_{out}^{\sharp A-1}$ and $u_{out}^{\sharp A-1}$ of PVDF ♯ A-1 and $v_{out}^{\sharp A-2}$, $s_{out}^{\sharp A-2}$ and $u_{out}^{\sharp A-2}$ of PVDF ♯ A-2 and differential output of v_{out}^{A}, s_{out}^{A} and u_{out}^{A} as follows:

$$*_{out}^{A} = *_{out}^{A-1} - *_{out}^{A-2} \qquad (* = v, s, u) \tag{10}$$

where A is constant of $A = 3, 4$.

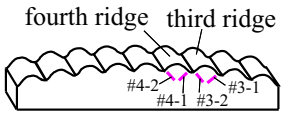

Figure 9: Definition of the PVDF transducers embedded in two ridges

The experimental result of the detected signal v_{out} is monitored when incipient slip occurs at the surface of finger skin as shown in **Figure 10**. In this figure, when the aluminum plate is slid in the x direction, low frequency components in signal v_{out} begin to increase. The arrows ↓ shows when the signal begin to increase. We refer to the signal in which low frequency components are dominant as *indication signal*. When incipient silp occurs on the surface of finger skin, the impulsive signal is monitored. The arrow ↑ shows when incipient slip occurs. We call the impulsive signal *slip signal*.

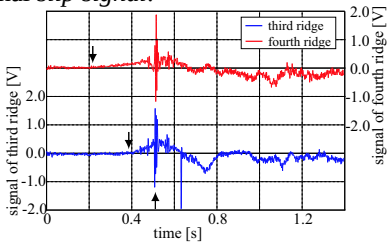

Figure 10: Differential output voltage signal v_{out} of the third and fourth ridges

Figure 11 shows the experimental result in which of s_{out} and u_{out} are monitored when incipient slip occurs. **Figure 11(a)** shows of s_{out} and **Figure 11(b)** shows of u_{out}. The result of s_{out} shows that the signal can pick up an *indication signal* pattern but cannot detect *slip signal*. On the other hand, the result of u_{out} shows that the signal can detect *slip signal* but cannot pick up the *indication signal*.

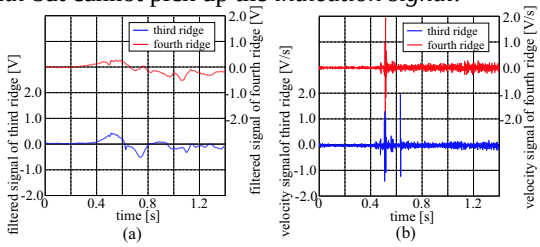

Figure 11: Differential output voltage signal: (a)filtered signal s_{out} (b)differential signal u_{out}

5.3 Strategy for detecting the incipient slip

In subsection **5.2**, we showed that not only *slip signal* but also *indication signal* could be monitored when incipient slip occurred at the surface of the artificial finger skin. We set a strategy for automatically detecting incipient slip as follows: First, *indication signal* is detected through monitoring s_{out}, while *slip signal* is through monitoring u_{out}. Second, if the two kinds of signal were detected, we judged that the incipient slip occurs at the skin surface. We do not use v_{out} because it is not capable of separate the *slip* and *indcation signals* from each other.

6 Judgment for occurrence of incipient slip

6.1 Method for the judgment

In order to judge whether any incipient slip occurs at the finger skin surface or not, we made an approach to use of multi-layered ANN(Artificial Neural Network). The architecture of the proposed for this judgment purpose ANN is shown in **Figure 12**. The output neurons of ANN are y_{slip} for incipient slip judgment, y_{non} for non-slip judgment and y_{ind} for possibility indication of incipient slip occurrence. The input neurons of ANN are s_{out}, u_{out} and y_{ind}. y_{ind} is a feedback element. Output y_{ind} is used for control of a robot hand which requires an *indication signal* of incipient slip occurrence to start increasing grasp force not to drop an object.

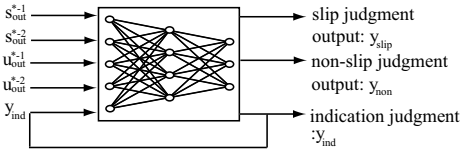

Figure 12: Structure of ANN with 5 input and 3 output neurons

6.2 Experimental result to judge the incipient slip

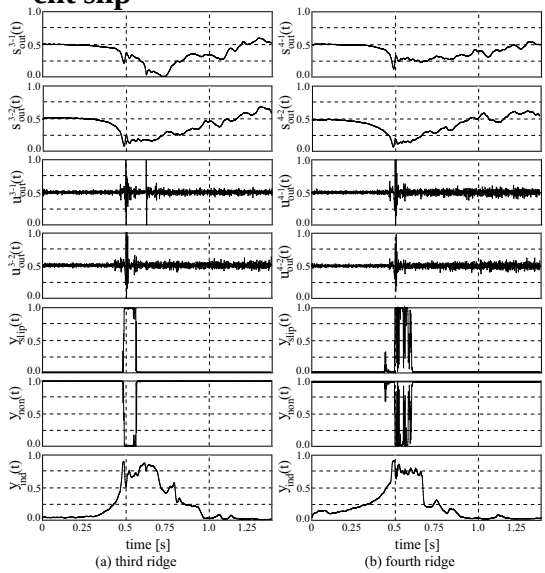

Figure 13: Result of judgment the incipient slip occurs

The experimental result for judgment of the incipient slip occurrence is shown in **Figure 13**. **Figure 13(a)** and **(b)** show the results of the judgment output signals in the third and fourth elements. The upper four figures show input signals of s_{out}^{A-1}, s_{out}^{A-2}, u_{out}^{A-1} and u_{out}^{A-2} where A denotes number of ridge shown in **Figure 9**. The third and second figures from the bottom depicts output signal of y_{slip} and y_{non}. The bottom figure traces y_{ind}. These results show the following: First, when an *indication signal* grows, signal y_{ind} starts to increase. This means that there is a possibility of incipient slip occurrence. Second, when an incipient slip occurs at the surface of the finger skin, which is shown as

Table 2: Experimental result of judgment of incipient slip and noise signals

	Slip judgment	Noise judgment
judgment[time]	6	0
non-judgment[time]	0	6

an impulse signal in the third and fourth figures, signal y_{slip} rises and indicates it with a certain peaked range. If a threshold voltage is set appropriately, and the amplitude of y_{slip} exceeds the threshold, the incipient slip occurring at the finger skin surface is exactly.

The statistical experimental result of judging incipient slip occurrence while some noise signal is also added purposely in different phases in an experiment is shown in **Table 2**. The slip judgment means whether the answer from y_{slip} exhibited a signal rise or not when either an actual slip phenomenon occurred or the signal was contaminated by some noise in each of 6 times of experiments. The result shows that in all experiments, the judgment signal made prefect answers and the result implies that the ANN system is also robust against noise signal.

7 Conclusion

In the paper, we described development of artificial finger skin with vibrotactile sensing elements based upon our design policy for verifying that incipient slip detection plays a central role for static friction sensing. The study is summarized in the following four items.

1. We showed design processes of artificial finger skin, which was followed by detailed design phases for attaining incipient slip detection.
2. We designed PVDF circuits and examined the frequency characteristics. We showed that the PVDF circuit displayed a stress rate characteristic, and modeled the equivalent circuit consisting of a parallely connected a resistance and a capacitance.
3. PVDF film strips were embedded in artificial finger skin and incipient slip was produced at the contact area with an object. We showed that such an incipient slip could be detected as follows; First, a low-frequency signal pattern was extracted for prediction of a incipient slip signal which might succeedingly occur. If such a predictive signal was monitored, we could attain successful detection of incipient slip. Finally, if the slip occurrence signal was detected, the grasping force of a robot hand could be increased to avoid dropping an object.
4. Multi-layered ANN technique was used in order to judge whether any incipient slip occurred or not. The output signals for slip judgment, non-slip judgment, and for indicating possibility of the incipient slip occurrence. The signal characteristic of having a first order bandpass filtering at 200 Hz peak frequency and the time derivative signal which is characteristic of stress acceleration. The other feedback signal was prepared as an input channel to indicate the occurrence. The experimental result shows that the indication signal began to increase when a low frequency signal pattern occurred, and y_{slip} rose to hit a peak when incipient slip occurred. From the result, we demonstrated that the proposed ANN system successfully detected the incipient slip occurrence.

Acknowledgments

We are indebted to Mr. Daisuke Yamada at Toyota Central Research and Development Laboratory Inc. for his helpful advice throughout this study. This study was supported by the Ministry of Education, Culture, Sports, Science and Technology under Grant-in-Aid for Scientific Research No.10450161.

References

[1] R. S. Johansson et al., Tactile sensory cording in the glabrous skin of the human hand, *Trends in NeuroSciences* ,Vol.6, No.1, pp27–32, 1983.

[2] G. Canepa et al., Detection of Incipient Object Slippage by Skin-Like Sensing and Neural Network Processing, *IEEE Transactions on Systems, Man, and Cybernetics-Part B: Cybernetics*, Vol.28, No.3, pp.348–356, 1998.

[3] M. R. Trembly et al., Estimating friction using incipient slip sensing during a manipulation task, *IEEE International conference on robotics and automation*, pp.429–434, 1993.

[4] J. S. Son et al., A Tactile Sensor for Localizing Transient Events in Manipulation, *Proceedings of 1994 Int. Conf. on Robotics and Automation*, pp.471–476, 1994.

[5] T. Maeno et al., FE Analysis of the Dynamic Characteristics of the Human Finger Pad in Contact with Objects with/without Surface Roughness, *Proc. 1998 ASME International Mechanical Engineering Congress and Exposition*, DSC-Vol.64, pp.279–286, 1998.

[6] Y. Yamada et al., Slip phase isolating : impulsive signal generating vibrotactile sensor and its application to real-time object regrip control, *Robotica*, Vol.18, pp.43–49, 2000.

[7] P. Dario et al., Piezoelectric Polymers: New Sensor Materials for Robotic Applications, *13th International Symposium on Industrial Robots and Robots 7*, Vol.2, pp.14-34–14-49, 1983.

[8] R. W. Patterson et al., The induced vibration touch sensor – a new dynamic touch sensing concept, *Robotica*, Vol.4, pp.27–31, 1986.

[9] R. D. Howe et al., Dynamic tactile sensing: Perception of fine surface features with stress rate sensing, *IEEE transactions on robotics and automation*, Vol.9, No.2, pp.140–151, 1993.

[10] Y. Yamada et al., Primary Development of Viscoelastic Robot Skin with Vibrotactile Sensation of Pacinian/ Non-Pachinian Channels, *Proceeding of the 3rd International Conference on Advanced Mechatronics*, pp.879–885, 1998.

[11] D. Yamada et al., Artificial Finger Skin having Ridges and Distributed Tactile Sensors used for Grasp Force Control, *Journal of Robotics and Mechatronics*,Vol.14, No.2, 2002.

[12] Delcomyn. Fred, *Foundation of Neurobiology. '97, W. H. Freeman*, 1997.

[13] Sergio Franco, *Design with Operational Amplifiers and Analog Integrated Circuits*, pp.28–33, *McGraw-Hill Book Company*, 1988